

ELECTRONIC SUPPLEMENTARY INFORMATION

Titania-coated gold nanorods with expanded photocatalytic response. Enzyme-like glucose oxidation under near-infrared illumination

M. C. Ortega-Liebana,^{a,b} J. L. Hueso,^{*a,b} R. Arenal,^c J. Santamaria,^{*a,b}

MATERIALS AND METHODS

Chemicals. Gold(III) chloride hydrate (50% Au basis), Hexadecyltrimethylammonium bromide (CTABr) (Sigma, 96%), sodium borohydride (Sigma, 99,99%), L-ascorbic acid (99%), 5-bromosalicylic acid (Sigma, 90%), silver nitrate (99.9999%), D-(+)-glucose (ACS reagent), Peroxidase from horseradish (type VI-A), 2,2-azino-bis (3-ethylbenzothiozoline)-6-sulfonic acid diammoniumsalt (ABTS-(NH₄)₂), 98% HPLC), 3,3',5,5'-Tetramethylbenzidine (TMB, 99%), Iron (III) chloride hexahydrate (97%), hydroxylamine solution (50wt% H₂O, 99.999%), trichloroacetic acid (99%), sodium bicarbonate (99.7-100%), Titanium (III) chloride solution (≥12% TiCl₃ basis, 12% in hydrochloric acid), Poly (sodium 4-styrenesulfonate (MW ≈ 70,000, powder), ethylenediaminetetraacetic acid (99,995%), triethylamine (98%), hydrochloric acid (37%), terephthalic acid 98% (TA) 9,10-Anthracenediyl-bis(methylene)dimalonic acid, Bio Reagent >90% (ABDA), pyridine anhydrous (99.8%), N,O-Bis (trimethylsilyl) trifluoroacetamide with 1% trimethylchlorosilane (BSTFA with 1%TMCS, for GC derivatization), methoxyamine hydrochloride (98%) and sodium hydroxide ACS reagent >97% were purchased from Sigma-Aldrich.

Preparation of gold nanorods. Bare Au NRs were synthesized following the seed-mediated method. Briefly, the seed solution was made by adding a freshly prepared,

ice-cold aqueous solution of NaBH_4 (0.6 mL, 0.01 M) into a mixture solution composed of $\text{HAuCl}_4 \cdot 3\text{H}_2\text{O}$ (29 μL , 0.086 M) and CTABr (10 mL, 0.1 M). The solution was stirred vigorously for 2 min and aged at room temperature for 30 min before use. The growth solution was prepared by dissolving CTAB (3.6 g) and 5-bromosalicylic acid (0.44 g) in 100 mL of warm water (Millipore, 55 °C). To this solution, 1.92 mL of 0.01 M fresh AgNO_3 was added, and after keeping it undisturbed at 25 °C for 15 min, 100 mL of 1 mM $\text{HAuCl}_4 \cdot 3\text{H}_2\text{O}$ solution was added. After gentle mixing of the solution for 15 min, 0.512 mL of 0.1 M ascorbic acid was added under vigorously stirring for 30 s until the mixture became colorless. At this point, 0.32 mL of seed solution was added to the entire growth solution. The mixture was stirred for 30 s and left undisturbed overnight at 27 °C.

Preparation of Au (noble metal nanocrystal core)/ TiO_2 (shell) nanostructures. The gold nanorods were first wrapped with PSS (molecular weight: $7 \times 10^4 \text{ g}\cdot\text{mol}^{-1}$). Typically, the initial solution (20 mL) of as-prepared gold nanorods was washed once by centrifugation to remove the excess of surfactant (CTABr) and then resuspended into water (10 mL). The resultant Au NRs solution was added dropwise under vigorous stirring to an aqueous PSS solution (10 mL, $4 \text{ g}\cdot\text{L}^{-1}$, containing 12 mM NaCl). PSS adsorption was allowed for at least 4 h at room temperature. The PSS excess and the displaced surfactant were removed by centrifugation and the PSS-encapsulated Au NRs were redispersed into water (400 μL). For the preparation of the (metal core)/(titania shell) nanostructures, TiCl_3 solution (150 μL , $\geq 12\%$, containing 12% in HCl) and water (6 mL) were first added into a glass bottle. NaHCO_3 solution (0.93 M, 0.9 mL) was then dropped, followed by the immediate addition of the PSS-encapsulated Au NRs solution

under stirring. After the mixture solution was stirred for 30 min at room temperature, the product was washed by centrifugation twice, re-dispersed in water (2 mL) and freeze dried before further use. The thermal treatment of core/shell nanostructures was carried out in a box furnace in air at 450 °C for 2 h with a ramp rate of 5 °C min⁻¹.

NIR-assisted glucose photo-oxidation mimicking reaction. Since the amount of enzyme mimic has a serious effect on the results, in order to investigate the glucose oxidase-mimicking AuNR-TiO₂ nanoparticles, we strictly controlled the amount of nanoparticles in the catalytic reactions. In a standard procedure, 0.02 mg mL⁻¹ nanoparticle were mixed with 10 mM D-glucose in 0.2 mol L⁻¹ sodium acetate buffer solution (pH = 7.4), in a total volume of 2 mL, which was irradiated (photocatalyst) with a red laser at 808 nm (1.5 W) using fiber collimation (THOLABSS F220SMA-780, 780nm, f=11.07mm). The initial reaction rates were calculated using the Lambert-Beer law. The absorbance values were back-calculated to yield total concentration using a molar absorption coefficient of 61.2 M⁻¹ cm⁻¹. This coefficient ϵ was previously determined from the slope of a linear fitting that correlated known concentrations of gluconic acid and the corresponding absorbance signal obtained upon the formation of the reddish hydroxamate-Fe(III)-complex.

Colorimetric assays for the detection of gluconic acid and hydrogen peroxide. The generation of gluconic acid was verified by reaction with hydroxylamine and subsequent complex with Fe^{III}, which led to a red complex hydroxamate-Fe³⁺ (with a maximum absorbance at 505 nm). In brief, 125 μ L of solution 1 (5 mmol·L⁻¹ EDTA and

0.15 mmol·L⁻¹ triethylamine in water) and 12.5 μL of solution 2 (3 mol·L⁻¹ NH₂OH in water) were added to 200 μL of the supernatant centrifuged reaction solution, and the mixture was allowed to react for 25 min. Finally, 62.5 μL of solution 3 (1 mol·L⁻¹ HCl, 0.1 mol·L⁻¹ FeCl₃, and 0.25 mol·L⁻¹ CCl₃COOH in water) was added to the reaction medium, and reaction was incubated for another 5 min before spectral acquisition. In order to prevent the influence of the nanoparticles, the solution was previously centrifuged at 6000 rpm in 2 mL eppendorf tubes. A systematic evaluation of the apparent steady-state kinetic parameters for the glucoxidase-like activity of the titania-coated Au NRs was carried out at different glucose concentrations (Figure 3a). The kinetics of the catalytic reaction could be adjusted to a typical Michaelis-Menten curve (Figure 3b). The Michaelis–Menten constant was calculated using the Lineweaver–Burk plot: $1/V_0 = (K_m/V_{max}) \cdot (1/[S]) + (1/V_{max})$, where V_0 is the initial velocity, V_{max} is the maximal reaction velocity, and $[S]$ is the concentration of the substrate. The rate of the catalytic reaction was defined as the amount of generated product, gluconic acid, in a fixed time interval of 30 min.

The other product, hydrogen peroxide (H₂O₂) was indirectly assayed with the aid of a horse radish peroxidase (HRP) enzyme that selectively favored the reduction of the H₂O₂ present in solution and the simultaneous oxidation of ABTS or TMB with specific absorbances at 415 and 652 nm, respectively. In a standard procedure, 300 μL of the filtered catalytic reaction solution was added to 50 μL of 8 mM ABTS and 50 μL of 0.4 μg mL⁻¹ HRP. The oxidation produced a green color with a major absorbance peak at 415 nm (final concentrations after dilutions for UV-Vis measurements were 1 mM ABTS and 0.05 μg mL⁻¹ HRP). Also, 350 μL of the filtered catalytic reaction solution was added to 8 μL of 40 mM TMB and 50 μL of 0.4 μg mL⁻¹ HRP (final concentrations after

dilutions for UV-Vis measurements were 0.8 mM TMB and 0.05 $\mu\text{g mL}^{-1}$ HRP). The oxidation produced a blue color with a major absorbance peak at 652 nm.

Detection of reactive oxidative species (ROS) generated upon NIR irradiation. The detection of singlet oxygen $^1\text{O}_2$ under laser irradiation (808 nm) was monitored using 9,10-anthracenediyl-bis(methylene) dimalonic acid (ABDA). Suspensions containing AuNRs or TiO_2 -coated Au NRs (0.02 mg mL^{-1}) were precipitated by centrifugation and redispersed in the presence of the probe molecule solutions. In a standard experiment for detecting $^1\text{O}_2$, ABDA (0.12 mM, 0.6 mL) was employed. To eliminate the adsorption effect of ABDA on the nanostructures, the mixture solution was first kept under stirring in dark for 4 h to reach adsorption equilibrium. Different aliquots were evaluated every ten minutes of laser irradiation after centrifugation. Furthermore, a thermostatic bath was also set at 19-20 $^\circ\text{C}$ to ensure a homogeneous suspension temperature and discard the influence of water evaporation events caused by local overheating of the solution. Likewise, the detection of hydroxyl radicals ($\bullet\text{OH}$) was carried out with the aid of terephthalic acid (TA, 3 mL, 5 mM) which selectively reacts to generate a fluorescent product (2-hydroxy terephthalic acid) emitting at ca. 425 nm. It is important to note that basic pH conditions (7-9) are first required to promote the stabilization of disodium terephthalate (NaTA). NaTA requires the neutralization of 790 mg of terephthalic acid with 50 mL of aqueous 0.05 M NaOH solution with constant stirring for 1 h. To separate the product, 8.3 g of NaOH were added to reach 14% by weight concentration. Under these conditions, the precipitate disodium terephthalate was filtered and finally dried in an oven at 110 $^\circ\text{C}$ for 12 hours. After laser illumination at different time intervals, the mixture solution was centrifuged to remove the catalyst

nanoparticles. The fluorescence emission spectrum of the generated 2-hydroxy disodium terephthalate in the supernatant was subsequently measured at an excitation wavelength of 315 nm.

Derivatization (methoxime-trimethylsilylation) for GC-MS analysis. Capped glass test tubes were used to carry out the derivatization process necessary in order to follow the reaction products by GC-MS. The derivatization process followed the guidelines given in previous reports¹⁻³. Catalytic reaction aliquots were centrifuged to separate the nanoparticles, after that 150 μ L of supernatant were transferred into a clean tube and freeze-dried. Methoximation was performed by adding 50 μ L of methoxyamine hydrochloride solution (20 mg/mL, pyridine solution) to the dried sample and then heating at 37 $^{\circ}$ C for 90 minutes. After that, trimethylsilylation was performed by adding 100 μ L of BSTFA with 1%TMCS and then heating at 37 $^{\circ}$ C for 30 minutes. The resulting solution was air dried and redissolved in 700 μ L ethyl acetate prior to GC/MS analysis.

Characterization techniques. The morphologies and particle size distributions were determined by transmission electron microscopy (TEM) (FEI Tecnai T20 and F30, operated at 200-300 kV, respectively). STEM-EELS studies have been developed using a FEI Titan Low-Base microscope, working at 80 kV. This microscope is equipped with a Cs probe corrector, a monochromator and an ultra-bright X-FEG electron source. The spectra were collected in STEM mode, using spectrum-image model. In the case of low-loss EELS, 15 spectra (of 1.3 ms/each) were acquired for each probe position

following a 2D region across the nano-object. It is worth noting that no evidence of irradiation damage in the sample was detected during the EEL spectra acquisition. The convergence and collection angle were 25 and 35 mrad., respectively. The energy resolution, after applying a deconvolution procedure based on the Richardson-Lucy algorithm ~ 170 meV. The tail of the zero-loss peak has been removed using a power law subtraction method⁴. To prepare the samples, the nanoparticle suspensions were diluted with water prior to casting on a holey carbon TEM grid. X-ray diffraction patterns were obtained in a PANalytical Empyrean equipment in Bragg-Brentano configuration using $\text{CuK}\alpha$ radiation and equipped with a PIXcel1D detector. The nanoparticles surface was analyzed by X-ray photoelectron spectroscopy (XPS) with an Axis Ultra DLD (Kratos Tech.). A monochromatic Al $\text{K}\alpha$ source (1486.6 eV) was employed with multiple runs at 12 kV, 10 mA and pass energy of 20 eV was used. The binding energies were calibrated to the internal C1s (284.2 eV) standard. Analyses of the peaks were performed with CasaXPS software, using a weighted sum of Lorentzian and Gaussian component curves after Shirley background subtraction. The size distribution of each sample was obtained through statistics over 200 particles. All measurements were performed at room temperature. ζ - Potential measurements were performed in KCl solution (0.1 M) (90 Plus, Brookhaven Instruments, Inc.). The GC-MS instrument used for the analysis was an GC-MS Shimadzu QP-2010SE system with an Zebron capillary GC column (30 m x 250 μm , 0.25 μm). The GC-MS instrument used for the analysis was a GC-MS Shimadzu QP-2010SE system equipped with a Zebron capillary GC column (30 m x 250 μm , 0.25 μm). NIST/EPA/NIH mass spectral library (NIST14) Helium (purity >99.999%) was used as a carrier gas with a flow rate of 1.0 ml min⁻¹, and a 1 μl sample was injected at a split mode. The temperature of

injection was set to 250 °C. The column temperature was first kept at 80 °C for 2 min, increased to 320 °C at a rate of 15 °C/min and maintained at 320 °C for 6 min. The detector was a quadrupole mass spectrometer and the temperatures of the ion source and interface were 200 and 250 °C, respectively.

SUPPLEMENTARY FIGURES

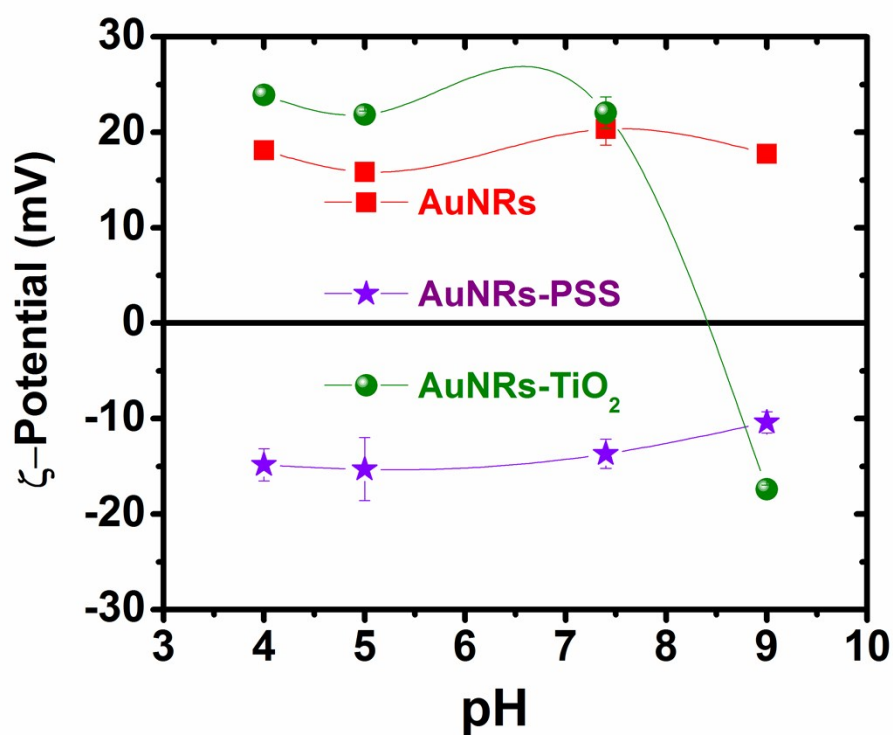


Figure S1. ζ -Potential at different pH values corresponding to the Au nanorods: as-prepared, after ligand exchange with PSS and after coating with titania.

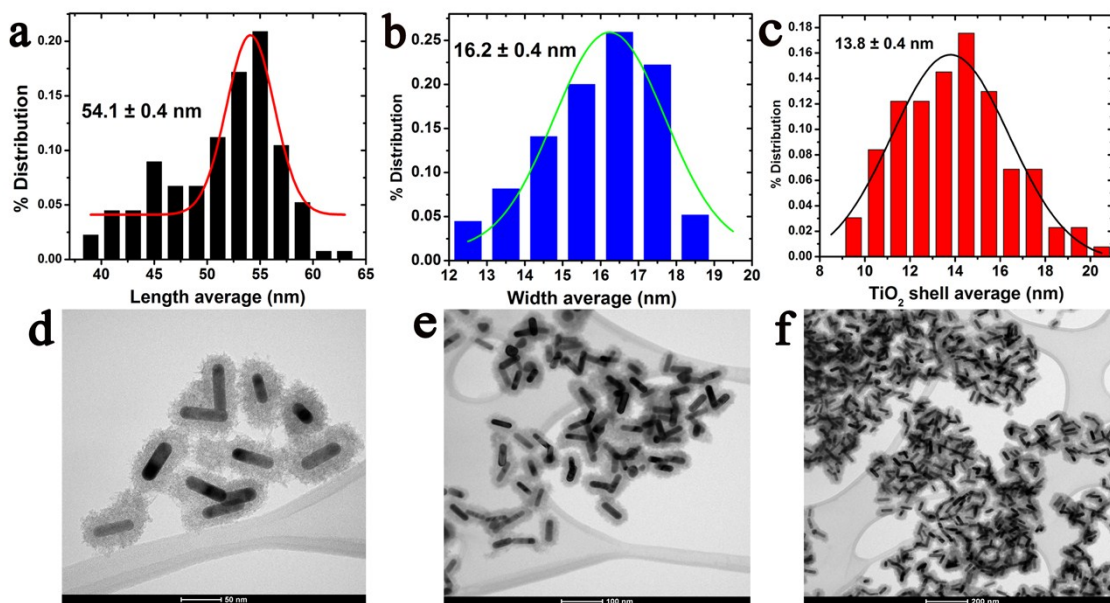


Figure S2. Particle size distribution of the gold nanorods: a) Length average; b) Width average; c) Average thickness of the titania shell; d)-f) Additional TEM images of the hybrid photocatalyst at different magnifications.

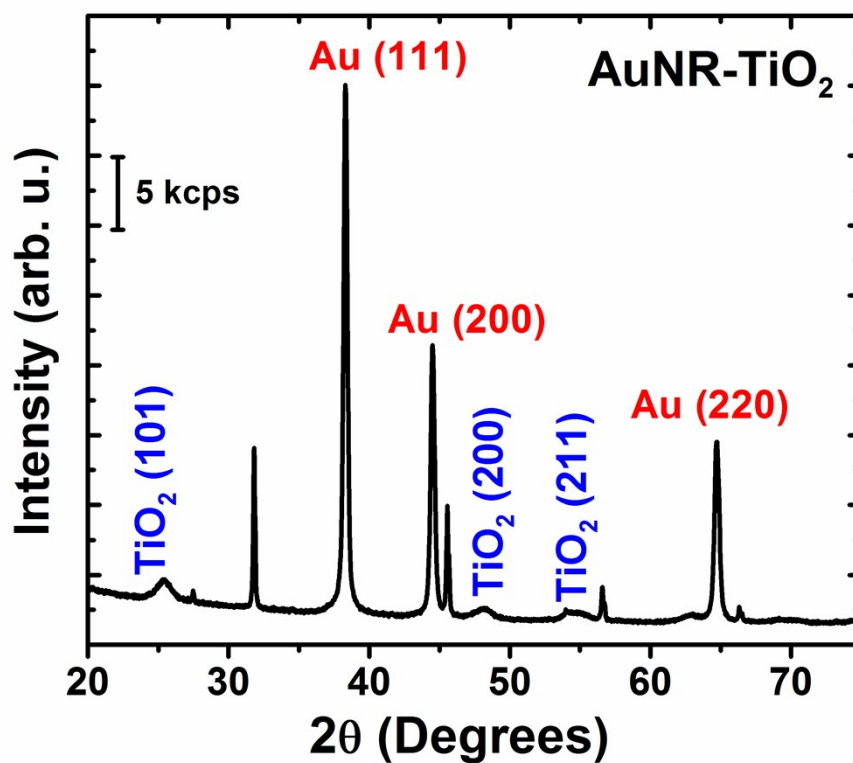


Figure S3. X-ray diffractogram of the titania-coated gold nanorods after calcination at 450 °C.

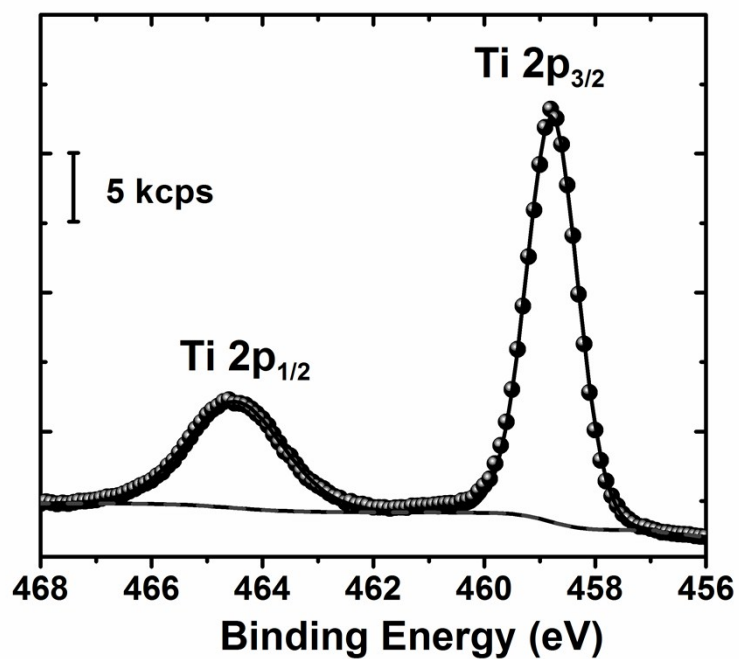


Figure S4. X-ray photoemission spectrum of the Ti2p region corresponding to the titania-coated gold nanorods after calcination at 450 °C.

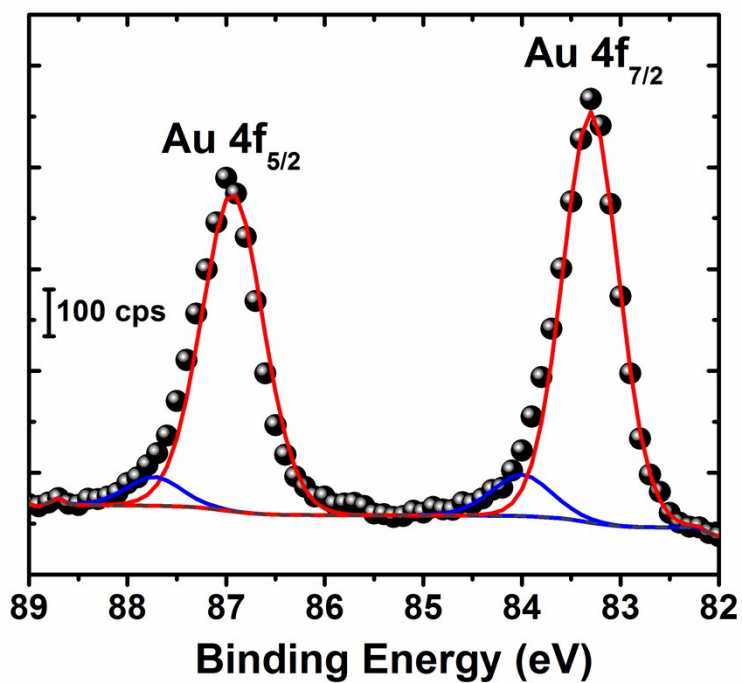


Figure S5. X-ray photoemission spectrum of the Au 4f region corresponding to the titania-coated gold nanorods after calcination at 450 °C.

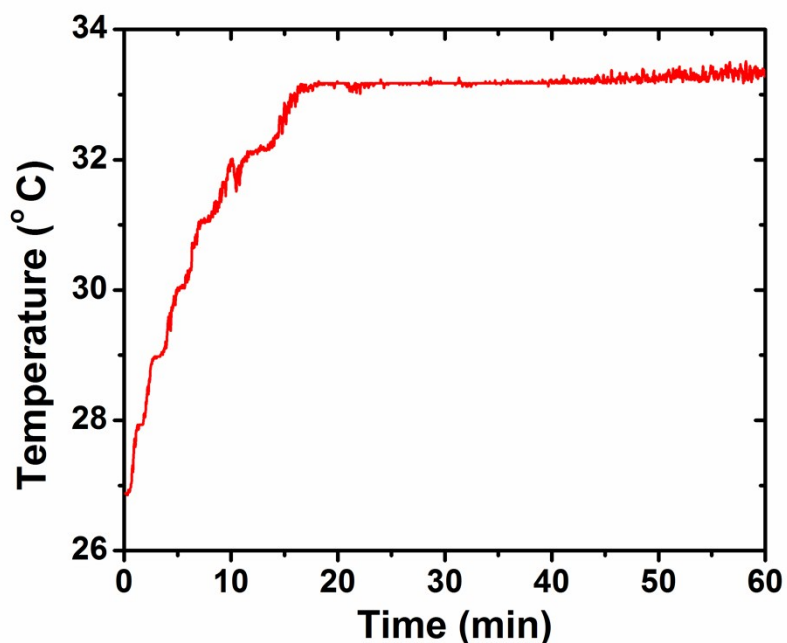


Figure S6. Temperature profile control during the NIR irradiation experiments to keep a constant value of 32-34 °C.

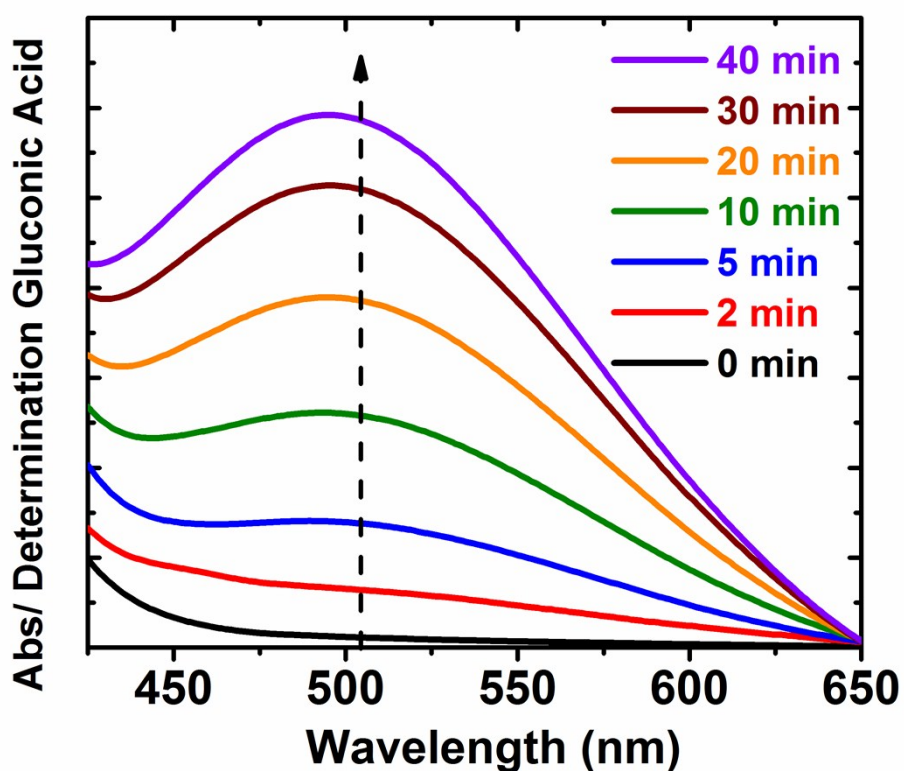


Figure S7. Relative absorbance values of the Fe-complex formed in the presence of the generated gluconic acid at increasing illumination times of the AuNR-TiO₂ core-shell photocatalyst. Experimental conditions: [glucose] = 10 mM; [catalyst] = 0.02 mg mL⁻¹; pH = 7.4 in 0.2 M NaAc buffer; Irradiation experiments with laser wavelength = 808 nm and laser power of 1.5 W; Reaction temperature: 33 °C.

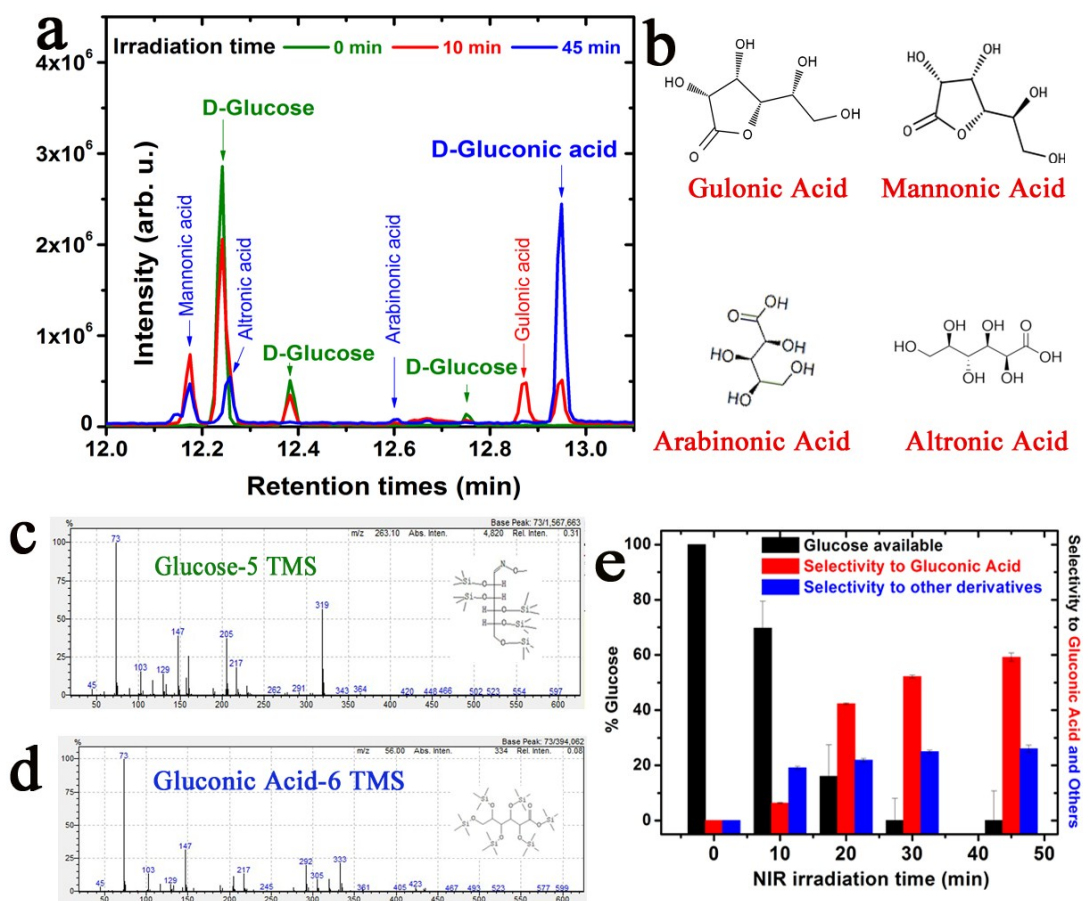


Figure S8: GC-MS analysis of the conversion of glucose in the presence of the Au-TiO₂ core-shell photocatalyst at different reaction times: a) Chromatograms displaying the evolution of glucose and the corresponding oxidation products before reaction and after NIR irradiation for 10 and 45 minutes, respectively; b) Chemical formulation of the main products identified other than gluconic acid; c)-d) Representative mass spectra patterns for methoxime-pentamethylsilylated D-glucose and methoxime-hexamethylsilylated D-gluconic acid, respectively; e) Evaluation of the cumulative glucose conversion and selectivity towards gluconic acid and other oxidation products at different irradiation times; Experimental conditions: [glucose] = 10 mM; [catalyst] = 0.02 mg mL⁻¹; pH = 7.4 in 0.2 M NaAc buffer; Irradiation experiments with laser wavelength = 808 nm and laser power of 1.5 W; Reaction temperature: 33-34 °C.

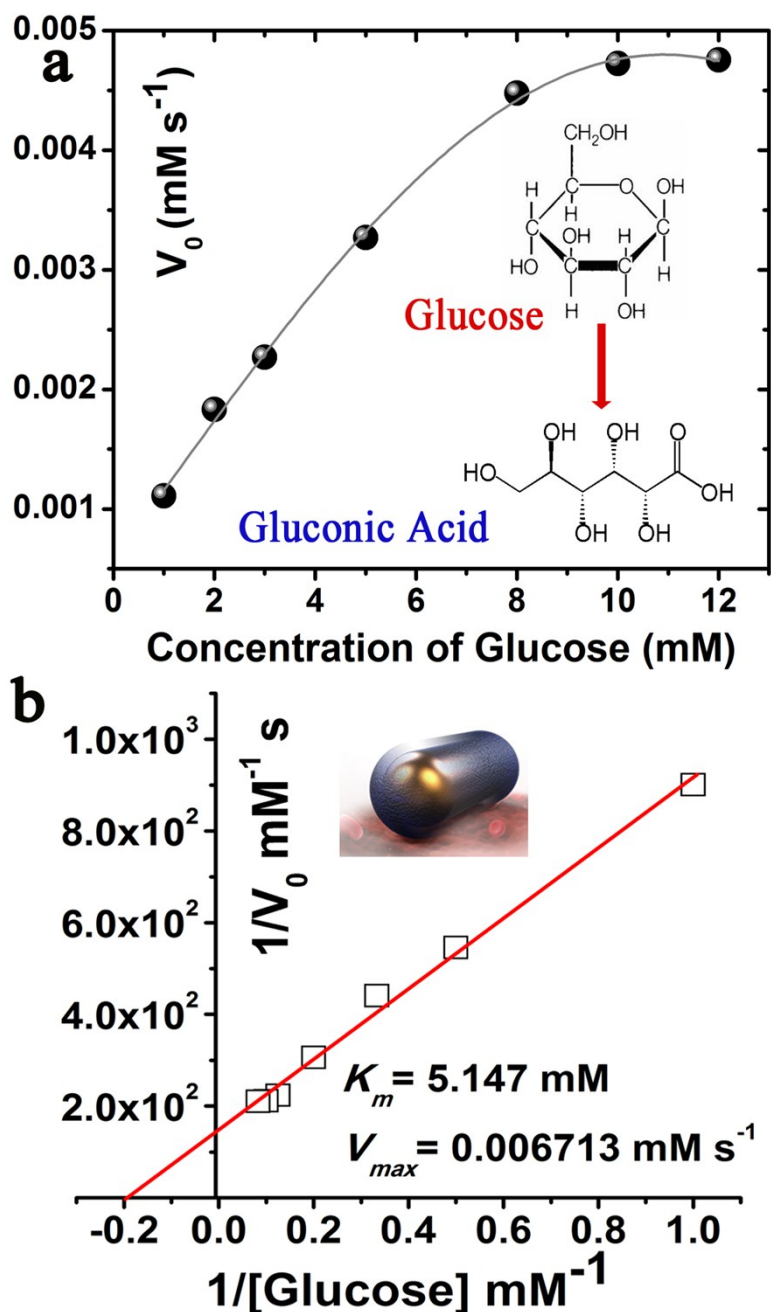


Figure S9. a) Steady-state kinetic assay and evaluation of the initial photo-induced conversion rates of glucose in the presence of the enzyme-like titania-coated Au NR photo-catalyst after 30 min of NIR laser irradiation using different substrate concentrations; b) Double-reciprocal plots of the glucose-oxidase mimicking activity after photo-irradiation of the core-shell catalyst assuming the Lineweaver-Burk fitting model. Experimental details: [glucose] = 1-12 mM; [catalyst] = 0.02 mg mL⁻¹; pH = 7.4 in 0.2 M NaAc buffer; Laser wavelength = 808 nm; Laser power = 1.5 W; Reaction temperature: 32-34 °C.

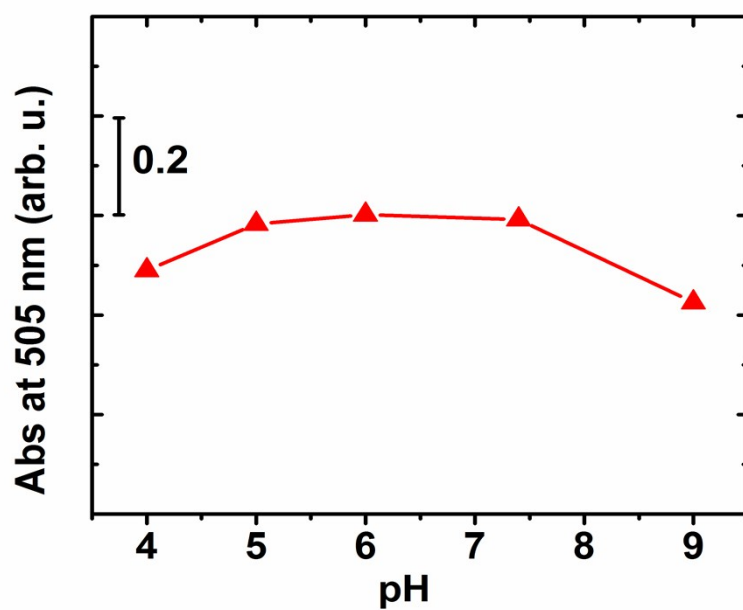


Figure 10. Influence of pH variations on the photocatalytic response of the titania-coated Au NR catalyst in the oxidation of glucose into gluconic acid. (Experimental conditions: [glucose] = 10 mM; [catalyst] = 0.02 mg mL⁻¹; pH = 4, 5, 6, 7.4, 9 in 0.2 M NaAc buffer; Laser wavelength = 808 nm; Laser power = 1.5 W; Reaction temperature: 32-34 °C.

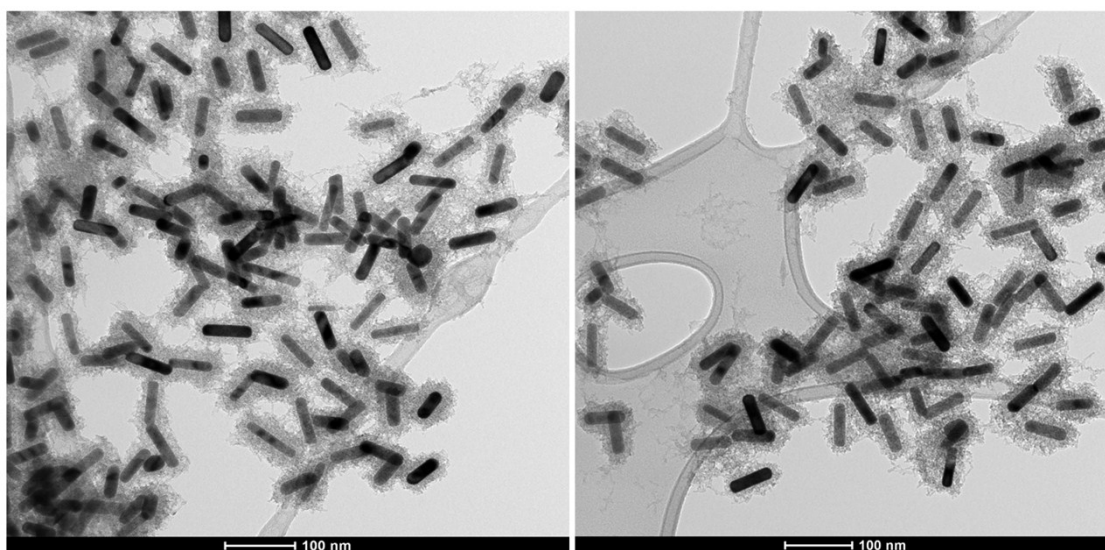


Figure S11. Representative TEM images of the titania-coated gold nanorod photocatalysts after 5 consecutive cycles of NIR illumination experiments.

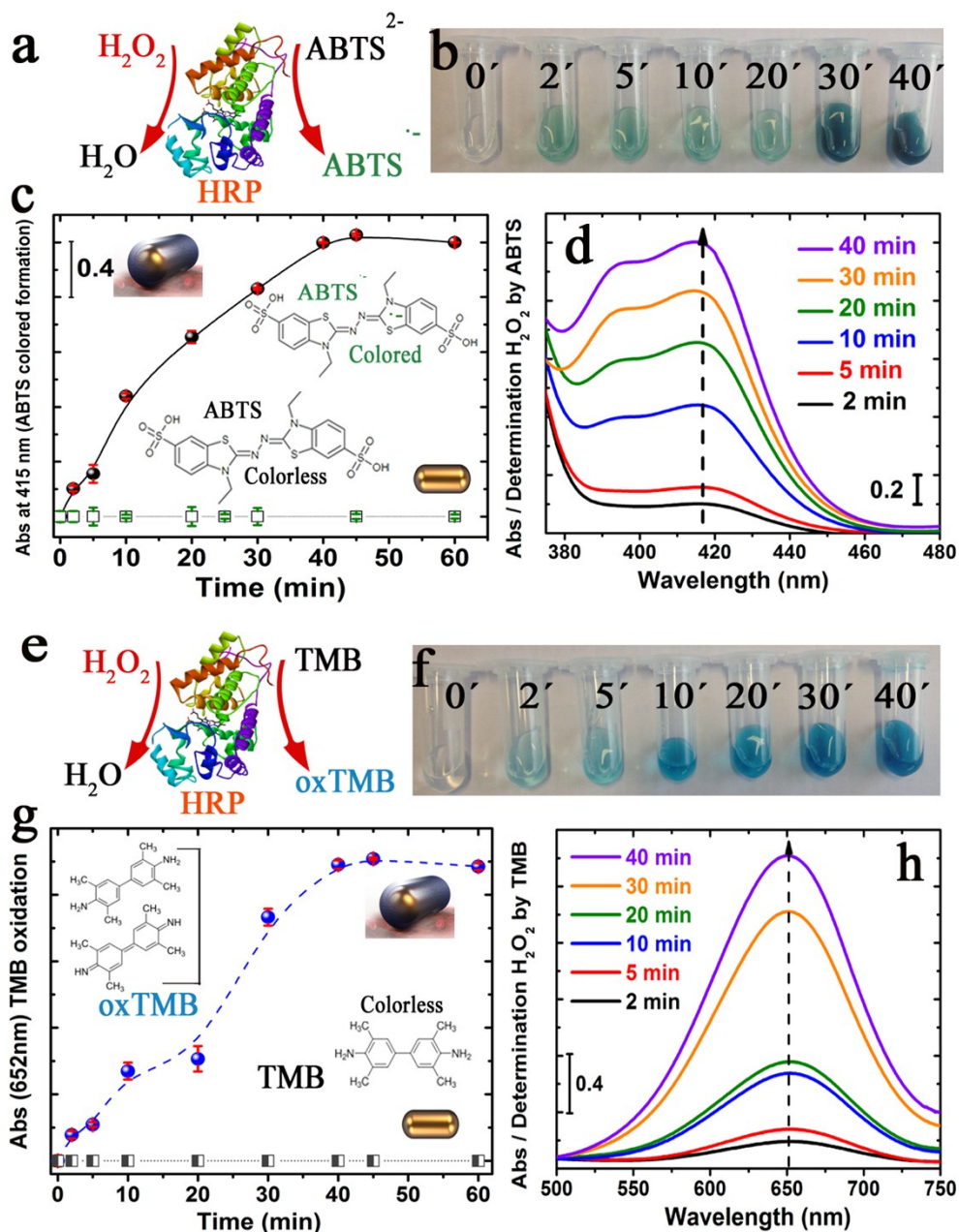


Figure S12. a) Schematic representation of the Horseradish Peroxidase (HRP) enzyme-promoted reduction of hydrogen peroxide with the simultaneous oxidation of ABTS to generate a colored complex absorbing at 415 nm; b) Digital photograph corresponding to different aliquots of oxidized ABTS after different NIR irradiation times up to 40 minutes in the presence of the AuNR-TiO₂ photocatalyst; c) Comparative evolution of the relative absorbance intensity of the ABTS^{•-} species detected by UV-Vis spectroscopy after different NIR illumination times in the presence of the titania-coated photocatalyst; d) Relative absorbance spectra of the in situ formed ABTS^{•-} species after different irradiation times in the presence of the titania-coated catalyst; e) Schematic representation of the HRP enzyme-promoted reduction of H₂O₂ and the simultaneous oxidation of TMB to generate an oxidized complex absorbing at 652 nm; f) Digital photograph corresponding to different aliquots of oxidized TMB after different NIR irradiation times up to 40 minutes in the presence of the AuNR-TiO₂ photocatalyst; g) Comparative evolution of the relative absorbance intensity of the oxidized TMB detected by UV-Vis spectroscopy after different NIR illumination time periods in the presence of the titania-coated photocatalyst; h) Relative absorbance spectra of the in situ formed oxidized TMB at different irradiation times in the presence of the titania-coated catalyst. Experimental details: [glucose] = 10 mM; [catalyst] = 0.02 mg mL⁻¹; pH = 7.4 in 0.2 M NaAc buffer; Laser wavelength = 808 nm; Laser power = 1.5 W; Reaction temperature: 32-34 °C; [HRP] = 0.05 μg mL⁻¹; [ABTS] = 1 mM; [TMB] = 0.8 mM.

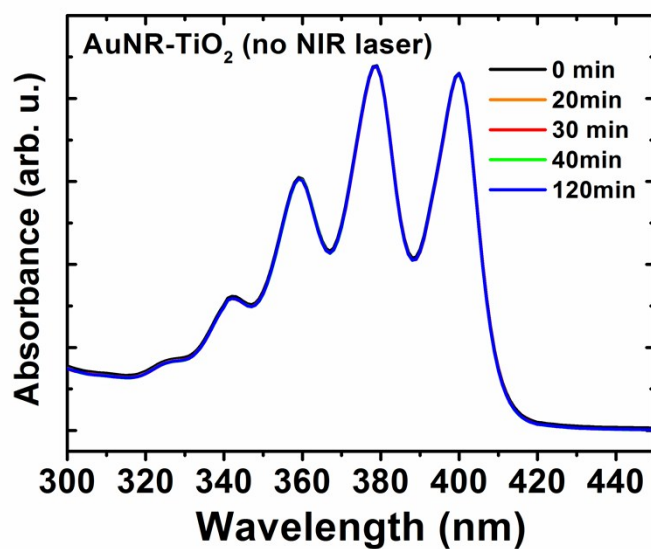


Figure S13. Control experiment to determine the potential generation of single oxygen species in the absence of NIR illumination. Similar results were obtained in analogous experiments carried out with bare Au NRs or after NIR irradiation without photocatalysts .

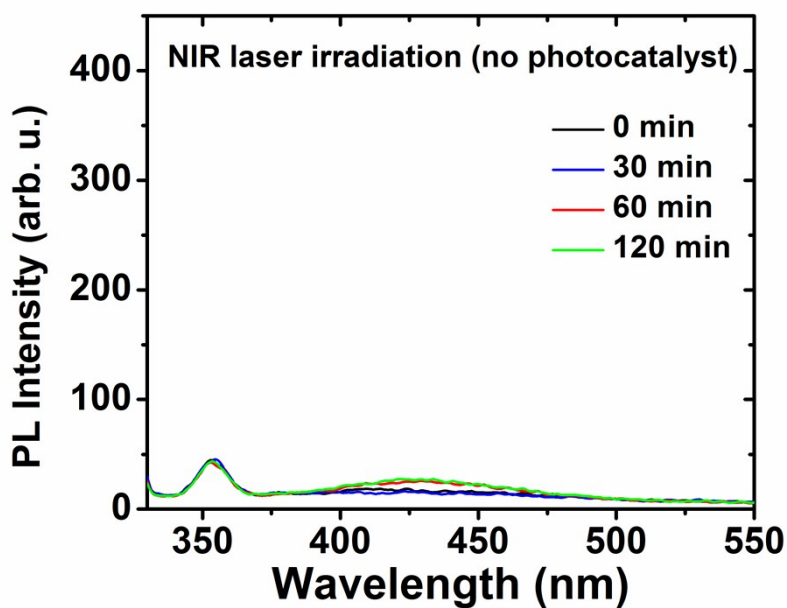


Figure S14. Control experiment for the determination of the hydroxyl radical generated in the absence of photo-catalysts under NIR illumination.

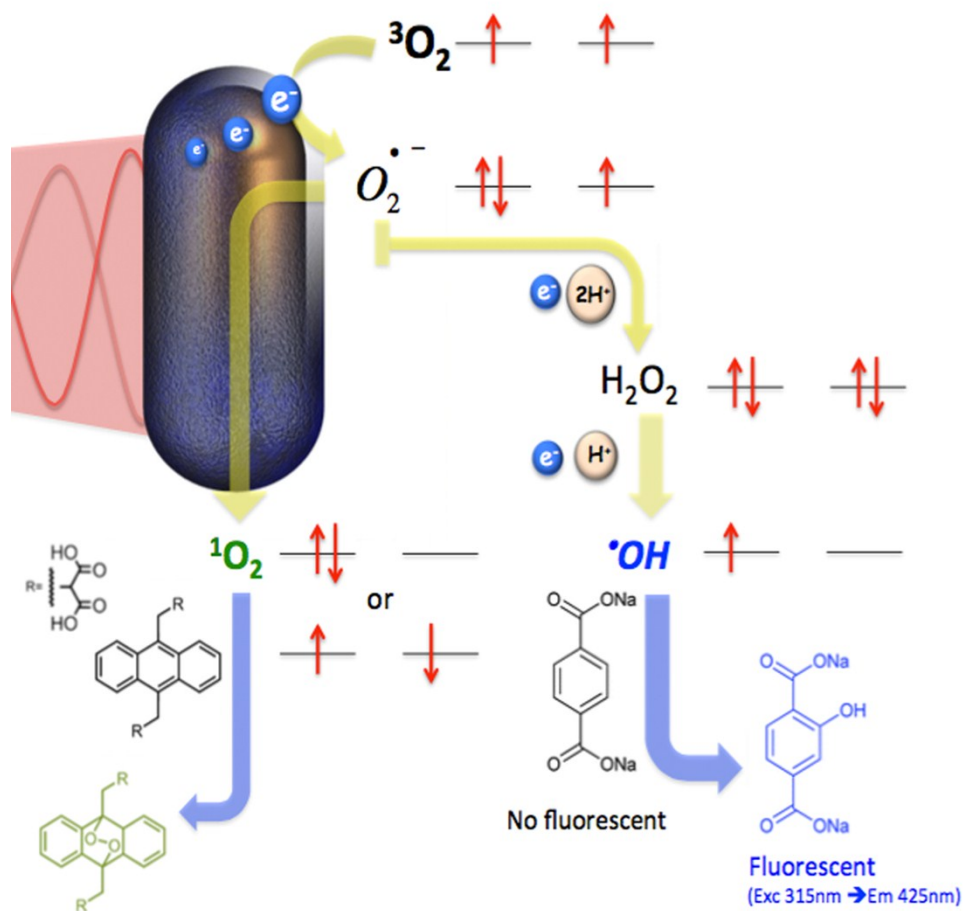


Figure S15. Schematic plot describing likely routes for the NIR-induced generation of ROS species such as singlet oxygen ($^1\text{O}_2$) or hydroxyl radicals ($\bullet\text{OH}$). The initiating step requires the formation of an effective Schottky barrier at the interface between the Au and TiO_2 . Plasmon excitation promotes the injection of hot electrons from gold into the conduction band of titania. These electrons favor the generation of superoxide anion radicals that readily react to form ($^1\text{O}_2$) or ($\bullet\text{OH}$) ROS that can be selectively probed against ABDA or NaTA, respectively.

SUPPLEMENTARY REFERENCES

1. S. Rautiainen, P. Lehtinen, M. Vehkamäki, K. Niemela, M. Kemell, M. Heikkilä and T. Repo, *Catal. Commun.*, 2016, **74**, 115-118.
2. A. I. Ruiz-Matute, O. Hernandez-Hernandez, S. Rodriguez-Sanchez, M. L. Sanz and I. Martinez-Castro, *J. Chromatogr. B*, 2011, **879**, 1226-1240.
3. P. N. Wahjudi, M. E. Patterson, S. Lim, J. K. Yee, C. S. Mao and W. N. P. Lee, *Clin. Biochem.*, 2010, **43**, 198-207.
4. R. F. Egerton, *Electron Energy-Loss Spectroscopy in the Electron Microscope* Plenum, New York, 1996.